ACS APPLIED MATERIALS & INTERFACES

Research Article

www.acsami.org

Highly Thermally Stable Single-Component White-Emitting Silicate Glass for Organic-Resin-Free White-Light-Emitting Diodes

Xuejie Zhang, Lin Huang, Fengjuan Pan, Mingmei Wu, Jing Wang,* Yan Chen, and Qiang Su

Ministry of Education Key Laboratory of Bioinorganic and Synthetic Chemistry, State Key Laboratory of Optoelectronic Materials and Technologies, KLGHEI of Environment and Energy Chemistry, School of Chemistry and Chemical Engineering, Sun Yat-sen University, Guangzhou, Guangdong 510275, P.R. China

Supporting Information

ABSTRACT: Thermal management is still a great challenge for high-power phosphor-converted white-light-emitting diodes (pc-WLEDs) intended for future general lighting. In this paper, a series of single-component white-emitting silicate SiO_2−Li_2O−SrO−Al_2O_3−K_2O−P_2O_5: Ce^{3+}, Tb^{3+}, Mn^{2+} (SLSAKP: Ce^{3+}, Tb^{3+}, Mn^{2+}) glasses that simultaneously play key roles as a luminescent convertor and an encapsulating material for WLEDs were prepared via the conventional melt-quenching method, and systematically studied using their absorption spectra, transmittance spectra, photoluminescence excitation and emission spectra in the temperature range 296−498 K, decay curves, and quantum efficiency. The glasses show strong and broad absorption in 250−380 nm region and exhibit intense white emission, produced by in situ mixing of blue-violet, green, and orange-red light from Ce^{3+}, Tb^{3+}, and Mn^{2+} ions, respectively, in a single glass component. The quantum efficiency of SLSAKP: 0.3%Ce^{3+}, 2.0%Tb^{3+}, 2.0%Mn^{2+} glass is determined to be 19%. More importantly, this glass shows good thermal stability, exhibiting at 373 and 423 K about 84.56 and 71.02%, respectively, of the observed room temperature (298 K) emission intensity. The chromaticity shift of SLSAKP: 0.3% Ce^{3+}, 2.0%Tb^{3+}, 2.0%Mn^{2+} is 2.94×10^{-2} at 498 K, only 57% of the commercial triple-color white-emitting phosphor mixture. Additionally, this glass shows no transmittance loss at the 370 nm emission of a UV-Chip-On-Board (UV-COB) after thermal aging for 240 h, compared with the 82% transmittance loss of epoxy resin. The thermal conductivity of the glass is about 1.07 W/mK, much larger than the 0.17 W/mK of epoxy resin. An organic-resin-free WLEDs device based on SLSAKP: 0.3%Ce^{3+}, 2.0% Tb^{3+}, 2.0%Mn^{2+} glass and UV-COB is successfully demonstrated. All of our results demonstrate that the presented Ce^{3+}/Tb^{3+}/Mn^{2+} tridoped lithium−strontium−silicate glass may serve as a promising candidate for high-power WLEDs.

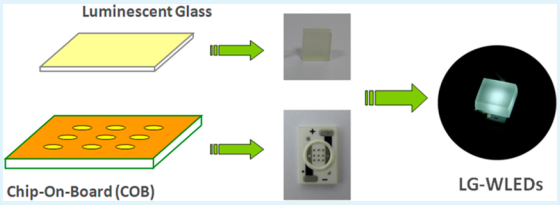

KEYWORDS: *white emission, luminescent glass, energy transfer, LG-WLEDs, organic-resin-free, high thermal stability*

1. INTRODUCTION

In recent years, high-power phosphor-converted white-light-emitting diodes (pc-WLEDs) have attracted more and more attention because they have been considered to be an alternative advanced lighting technology to conventional incandescent and fluorescent lamps for future general lighting.[1−6]

To date, the input current of high-power InGaN-based LED chips with a power of more than 3 W used as pump excitation source in pc-WLEDs has typically been in the 350/750/1000 mA range.[7] Besides high luminous flux, a high input current or high power leads to high local heat flux in InGaN-based LED chips. The junction temperature of these chips is now as high as 150−200 °C.[8] Such a high junction temperature inevitably causes serious degradation of the InGaN-based LED chips used as the pump excitation source, the rare earth phosphor used as luminescent convertor, and the organic resin used as encapsulating material, the three critical components in pc-WLEDs.[9] In detail, a high junction temperature can result in a decrease in luminous efficiency of LED chips as well as obvious wavelength shift of their dominant emission, an order of magnitude reduction of the phosphor emission due to the thermal quenching effect, serious decreases in optical transmittance caused by the yellowing and carbonizing of the organic resin because of chemical bond breakage. Thus, the optical performance of pc-WLEDs, such as luminous efficiency and chromaticity, deteriorates after a period of operation and the lifetime of pc-WLEDs shortens.[7,9,10] In summary, thermal management has become an urgent and hot issue as a great challenge for the fabrication of high-power pc-WLEDs for future general lighting.

Luminescent glasses are important materials with excellent thermal resistance, and can simultaneously play the same key roles of luminescent convertor and encapsulating material as the conventional phosphor powder and organic resin, respectively, used in pc-WLEDs. Moreover, they do not exhibit the light scattering loss of the traditional slurry mixed with phosphor and organic resin, caused by the large difference in refractive index between them,[11] and can give homogenously emitted light, which is too difficult to realize in traditional slurry

Received: November 19, 2013
Accepted: January 27, 2014
Published: January 27, 2014

   dx.doi.org/10.1021/am405228x | ACS Appl. Mater. Interfaces 2014, 6, 2709−2717

because of the nonuniform dispersion of phosphor in the organic resin.[12] Therefore, luminescent glass based WLEDs (LG-WLEDs) are strongly expected to be an interesting and excellent alternative approach to traditional pc-WLEDs fabricated by combining InGaN-based LED chips, with phosphor and organic resin.

Recently, many efforts have been made to develop luminescent glasses for LG-WLEDs.[13−16] In 2005, Fujita and Tanabe reported excellent thermal resistance properties for glass-ceramic YAG: Ce^{3+} and demonstrated its application in WLEDs.[17,18] However, this WLEDs still suffered from a low color-rendering index (CRI) and high correlated color temperature (CCT) because of a scarcity of red emission. In 2012, Li and da Cunha Andrade et al. reported Eu^{2+}-doped low-silica calcium aluminosilicate (LSCAS) glass, with broad and intense orange-red light emission and the maximum luminescence quantum efficiency reported in the literature was about 50%.[19,20] Unfortunately, it is very difficult to improve CRI and decrease CCT by simply combining YAG: Ce^{3+} glass-ceramic and LSCAS: Eu^{2+} glass in LG-WLEDs like the phosphors in pc-WLEDs. Therefore, many tridoped systems were reported, including Tm^{3+}-Tb^{3+}-Mn^{2+}-tridoped glass or glass-ceramic,[21,22] Ce^{3+}-Tb^{3+}-Sm^{3+}-tridoped glass,[23] Ce^{3+}-Tb^{3+}-Eu^{3+}-tridoped glass,[24,25] and Ce^{3+}-Tb^{3+}-Mn^{2+}-tridoped glass.[26−28] However, some of these glasses are poor in mechanical and chemical stability, some cannot be excited effectively because of weak f−f absorption, and others are not very suitable for UV-LED chips ascribed to their maximum excitation wavelengths in deep UV.

In this paper, we report for the first time single-composition tunable white-emitting SLSAKP: Ce^{3+}, Tb^{3+}, Mn^{2+} glasses, and discuss in detail the energy transfer from Ce^{3+} to Tb^{3+} and Mn^{2+}. In addition, the thermal quenching properties of SLSAKP: 0.3%Ce^{3+}, 2.0%Tb^{3+}, 2.0%Mn^{2+} glass were also investigated. The heat-resistance, thermal-induced degradation, and thermal conductivity properties of the SLSAKP: 0.3%Ce^{3+}, 2.0%Tb^{3+}, 2.0%Mn^{2+} glass were compared with those of epoxy resin. As-fabricated LG-WLEDs was also successfully demonstrated.

2. EXPERIMENTAL SECTION

2.1. Sample Preparation. SLSAKP and SLSAKP: $x$$Ce^{3+}$, $y$$Tb^{3+}$, $z$$Mn^{2+}$ glasses were prepared by the conventional melt-quenching method. The mother glass had a composition (mol %) of $45SiO_2$−$30Li_2O$−$15SrO$−$5Al_2O_3$−$3K_2O$−$2P_2O_5$. The raw materials were analytical purity SiO_2, Al_2O_3, Li_2CO_3, $SrCO_3$, K_2CO_3, $MnCO_3$, and $NH_4H_2PO_4$, and high-purity rare earth oxides CeO_2 (4N) and Tb_4O_7 (4N). The chosen mixtures of the corresponding raw materials were thoroughly ground with an agate mortar and pestle, and then melted in corundum crucibles at 1500 °C for 90 min in thermal-carbon reducing atmosphere. The melts were cast into preheated (500 °C) graphite molds and annealed in a muffle furnace at 500 °C for 2 h in ambient atmosphere to relieve the internal stress. Finally, they were cooled to room temperature. The as-synthesized glasses were cut and carefully polished into specimens of ∼3 mm thickness to meet the requirements for optical measurements. Each side of the as-synthesized glass was lapped with emery of about 400 Mesh for 10 min in a rough-polishing process. The triple-color phosphor mixture was made by appropriately adjusting the ratio of commercial $BaMgAl_{10}O_{17}$: Eu^{2+} (blue), $(Ba,Sr)_2SiO_4$: Eu^{2+} (green) and Y_2O_2S: Eu^{3+} (red) phosphors. The epoxy resin plate (∼2 mm) was composed of IK0010(A) and IK0010(B) epoxy (ratio of A to B is 1:1). The COB LED modules consisted of a 3 × 3 array of UV (∼370 nm) chips.

2.2. Measurements and Characterization. Absorption and transmittance spectra were recorded with a Cary 5000 UV−vis−NIR spectrophotometer (Varian) equipped with double out-of-plane Littrow monochromator. The photoluminescence excitation (PLE) and photoluminescence (PL) spectra within the temperature range 296−498 K as well as the decay curves were measured using an Edinburgh Instruments FSP920 time-resolved and steady -state fluorescence spectrometers equipped with a 450 W Xe lamp, a 150 W nF900 flash lamp, TM300 excitation monochromator and double TM300 emission monochromators and thermoelectric cooled red-sensitive PMT. The spectral resolution of the steady measurements was about 0.05 nm in UV−vis. The sample was mounted in an Oxford OptistatDN2 nitrogen cryostat for PLE and PL measurements above room temperature. The room temperature quantum efficiency (QE) of the sample was measured using a barium sulfate coated integrating sphere (150 mm in diameter) attached to the FSP920. Epoxy resin was chosen as a reference to test thermal-resistance. The aging temperature was set at 150 °C. The epoxy resin plate and SLSAKP: 0.3%Ce^{3+}, 2.0% Tb^{3+}, 2.0%Mn^{2+} glass were exposed at 150 °C in the oven for the prescribed time period. The thermal conductivity was measured using a Hot Disk TPS 2500 Thermal Constants Analyzer. Electroluminescence (EL) spectra were recorded at a forward-current and measured using an Ocean Optics Instruments QE65000.

3. RESULTS AND DISCUSSION

3.1. Spectroscopic Properties of SLSAKP: $x$$Ce^{3+}$, $y$$Tb^{3+}$, $z$$Mn^{2+}$ Glasses. Figure 1 shows the absorption spectra of the

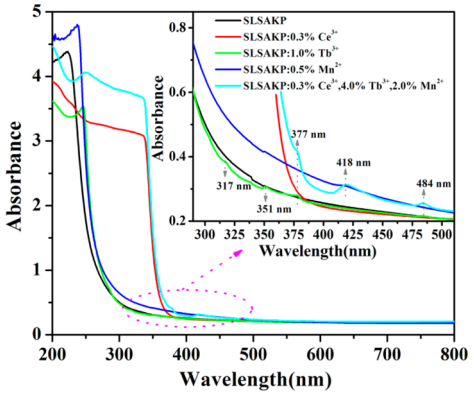

Figure 1. Absorption spectra of SLSAKP, SLSAKP: 0.3%Ce^{3+}, SLSAKP: 1.0%Tb^{3+}, SLSAKP: 0.5%Mn^{2+}, and SLSAKP: 0.3%Ce^{3+}, 4.0%Tb^{3+}, 2.0%Mn^{2+} glasses. The inset is the magnification of the absorption spectra in the range 300−500 nm.

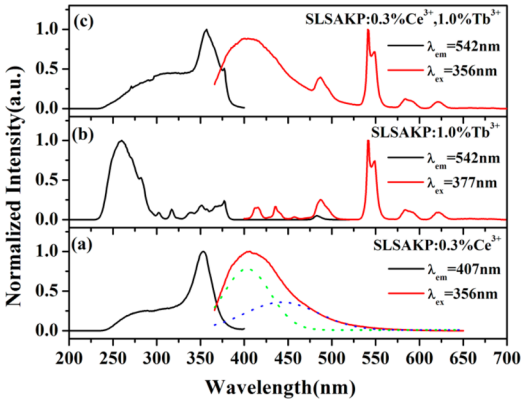

Figure 2. PLE and PL spectra of (a) SLSAKP: 0.3%Ce^{3+}, (b) SLSAKP: 1.0%Tb^{3+}, and (c) SLSAKP: 0.3% Ce^{3+}, 1.0% Tb^{3+} glasses. The Gaussian fitting sub-bands of the emission curve of the SLSAKP: 0.3%Ce^{3+} glass are also shown in a.

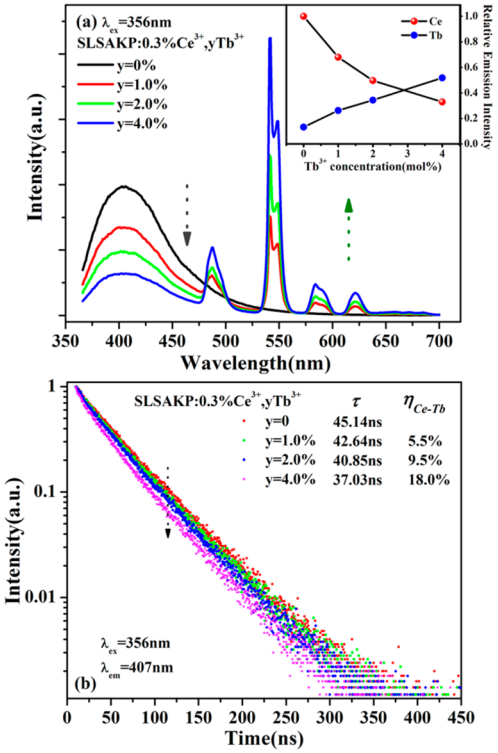

Figure 3. (a) PL spectra (λ_{ex} = 356 nm) of SLSAKP: 0.3%Ce^{3+}, yTb^{3+} (y = 0, 1.0, 2.0, 4.0%). The inset shows the dependence of the PL intensities of Ce^{3+} and Tb^{3+} on Tb^{3+} concentration in SLSAKP: 0.3% Ce^{3+}, yTb^{3+}. (b) Decay curves (λ_{ex} = 356 nm, λ_{em} = 407 nm) of Ce^{3+} in SLSAKP: 0.3%Ce^{3+}, yTb^{3+} (y = 0, 1.0, 2.0, 4.0%).

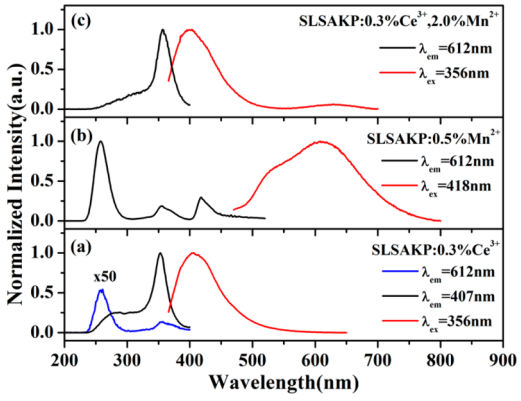

Figure 4. PLE and PL spectra of (a) SLSAKP: 0.3%Ce^{3+}, (b) SLSAKP: 0.5%Mn^{2+}, and (c) SLSAKP: 0.3%Ce^{3+}, 2.0%Mn^{2+} glasses.

obtained SLSAKP, SLSAKP: 0.3%Ce^{3+}, SLSAKP: 1.0%Tb^{3+}, SLSAKP: 0.5%Mn^{2+} and SLSAKP: 0.3%Ce^{3+}, 4.0%Tb^{3+}, 2.0% Mn^{2+} glasses. The SLSAKP glass has only a strong absorption band below 250 nm, ascribed to its intrinsic host absorption. The SLSAKP: 0.3%Ce^{3+} glass exhibits an intense broadband absorption from 250 to 380 nm, because of the allowed 4f→5d transition of Ce^{3+} ions. Compared with the host glass, the absorption edge of the SLSAKP: 0.3%Ce^{3+} shows an obvious red-shift from ~264 to ~365 nm. For the SLSAKP: 1.0%Tb^{3+} glass, there are several weak sharp peaks at around 317, 351, 377, and 484 nm, attributed to the forbidden $^7F_6$→($^5H_7$, $^5D_{0,1}$), $^7F_6$→($^5L_9$, $^5G_4$), $^7F_6$→($^5D_3$, $^5G_6$), and $^7F_6$→$^5D_4$ transitions of Tb^{3+} ions, respectively, as shown in the inset of Figure 1.[29] For the SLSAKP: 0.5%Mn^{2+} glass, one weak sharp peak at about

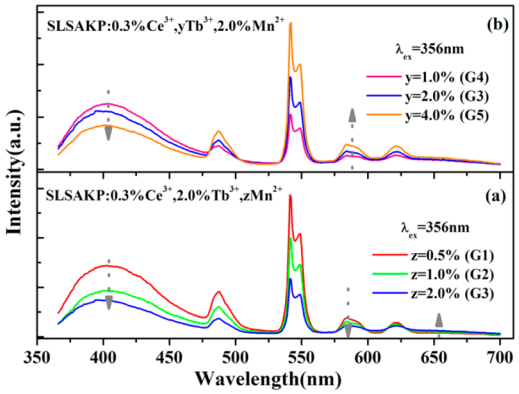

Figure 5. PL spectra (λ_{ex} = 356 nm) of SLSAKP: 0.3% Ce^{3+}, yTb^{3+}, zMn^{2+} glasses (G1: y = 2.0%, z = 0.5%; G2: y = 2.0%, z = 1.0%; G3: y = 2.0%, z = 2.0%; G4: y = 1.0%, z = 2.0%; G5: y = 4.0%, z = 2.0%).

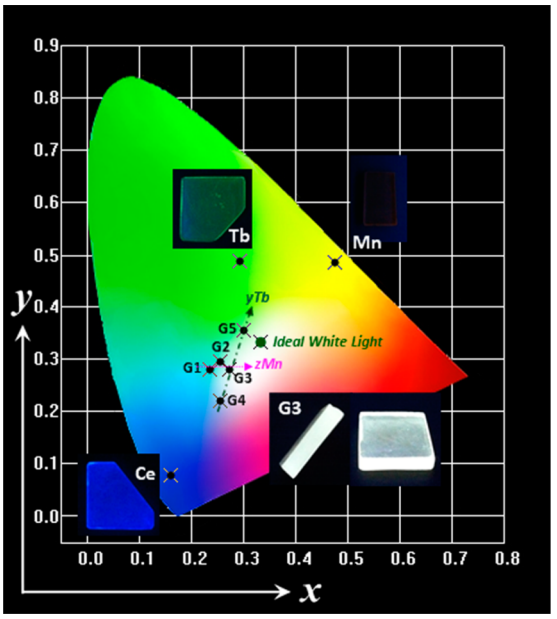

Figure 6. CIE chromaticity diagram of SLSAKP: 0.3%Ce^{3+}, SLSAKP: 1.0%Tb^{3+}, SLSAKP: 0.5%Mn^{2+}, and SLSAKP: 0.3%Ce^{3+}, yTb^{3+}, zMn^{2+} glasses (G1: y = 2.0%, z = 0.5%; G2: y = 2.0%, z = 1.0%; G3: y = 2.0%, z = 2.0%; G4: y = 1.0%, z = 2.0%; G5: y = 4.0%, z = 2.0%). Inset shows digital photographs of SLSAKP: 0.3%Ce^{3+}, SLSAKP: 1.0%Tb^{3+}, SLSAKP: 0.5%Mn^{2+}, and SLSAKP: 0.3%Ce^{3+}, 2.0%Tb^{3+}, 2.0%Mn^{2+} glasses under 365 nm UV lamp irradiation.

418 nm, assigned to the forbidden $^6A_1(S)$ → $^4A_1(G)$, $^4E(G)$ transitions, is carefully observed in the inset of Figure 1. The absorption spectrum of the tridoped SLSAKP glass shows the same characteristic features of all ions, Ce^{3+}, Tb^{3+}, and Mn^{2+}, as those of the single ion-doped glasses.

Figure 2 shows the PLE and PL spectra of SLSAKP: 0.3% Ce^{3+}, SLSAKP: 1.0%Tb^{3+} and SLSAKP: 0.3%Ce^{3+}, 1.0%Tb^{3+} glasses. As shown in Figure 2a, the PLE spectrum shows a broad band from 250 to 380 nm, assigned to the allowed transitions from the ground state to the crystal-field splitting levels of the $5d^1$ state of Ce^{3+}. The intense excitation broadband of Ce^{3+} in this glass matches well with the emitted light of the UV-LED chips. Under excitation at 356 nm, SLSAKP: 0.3% Ce^{3+} shows an asymmetric emission band (370−500 nm) with a maximum at 407 nm, ascribed to the $4f^05d^1$→$4f^1$ transitions of Ce^{3+}. The emission band was deconvoluted into two well-

dx.doi.org/10.1021/am405228x | ACS Appl. Mater. Interfaces 2014, 6, 2709−2717

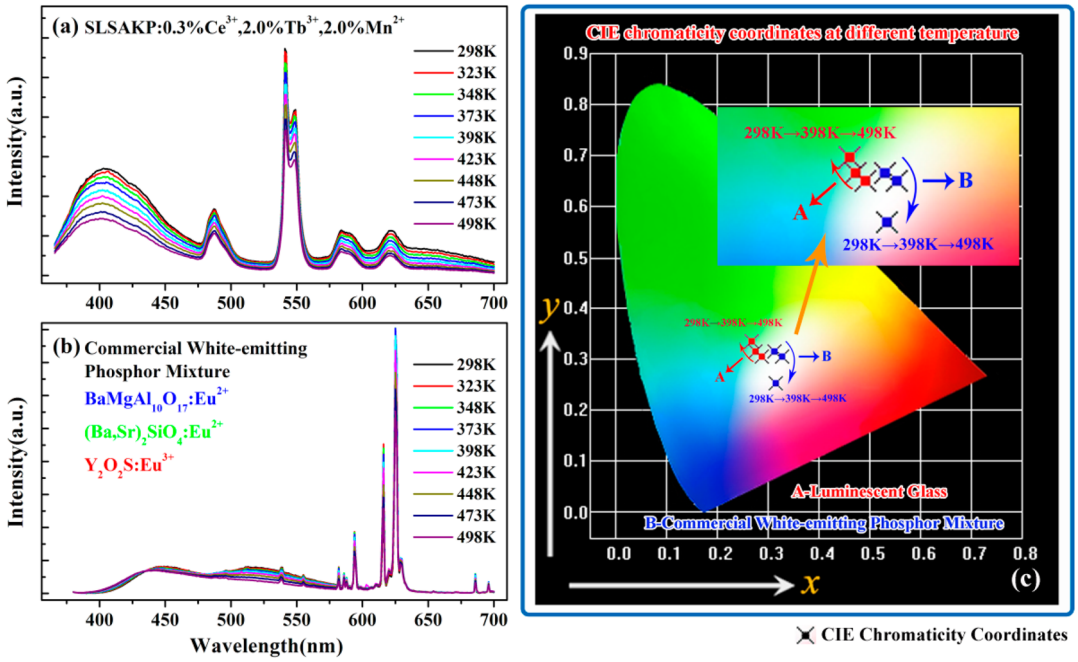

Figure 7. PL spectra of the (a) SLSAKP: 0.3%Ce^{3+}, 2.0%Tb^{3+}, 2.0%Mn^{2+} glass (λ_{ex} = 356 nm) and (b) commercial white-emitting phosphor mixture (λ_{ex} = 370 nm) in the temperature range 298−498 K. (c) Variation in CIE chromaticity coordinates at different temperatures (red star: SLSAKP: 0.3%Ce^{3+}, 2.0%Tb^{3+}, 2.0%Mn^{2+} glass; blue star: commercial white-emitting phosphor mixture).

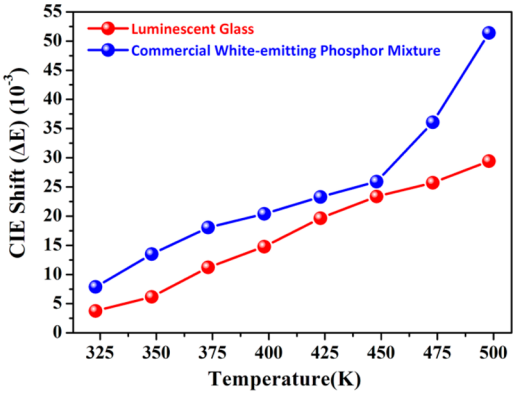

Figure 8. Chromaticity shift of the SLSAKP: 0.3%Ce^{3+}, 2.0%Tb^{3+}, 2.0%Mn^{2+} glass (λ_{ex} = 356 nm) and the commercial white-emitting phosphor mixture (λ_{ex} = 370 nm) as a function of temperature.

separated Gaussian components at 404 and 444 nm, attributed to the 5d→$^2F_{5/2}$ and 5d→$^2F_{7/2}$ transitions, respectively. The energy difference between these two sub-bands was calculated to be ∼2230 cm^{-1}, which is close to the theoretical value of ∼2000 cm^{-1}.[30] As shown in Figure 2b, the SLSAKP: 1.0%Tb^{3+} glass exhibits a broad excitation band at 264 nm and some sharp peaks in the range 300−500 nm. The former is caused by the allowed $4f^8$→$4f^75d^1$ transition of Tb^{3+} while the latter are derived from its intra-(4f) transitions. Under 377 nm excitation, the emission spectrum shows the characteristic optical transitions of Tb^{3+} at about 414, 434, 458, 486, 542, 585, and 620 nm, due to $^5D_3$→$^7F_5$, $^5D_3$→$^7F_4$, $^5D_3$→$^7F_3$, $^5D_4$→$^7F_6$, $^5D_4$→$^7F_5$, $^5D_4$→$^7F_4$, and $^5D_4$→$^7F_3$, respectively. The existence of a spectral overlap between the emission spectrum of SLSAKP: 0.3%Ce^{3+} and the excitation spectrum of SLSAKP: 1.0%Tb^{3+} is obvious, indicating that an energy transfer may occur in the SLSAKP host, where Ce^{3+} and Tb^{3+} ions act as energy donor and acceptor, respectively.

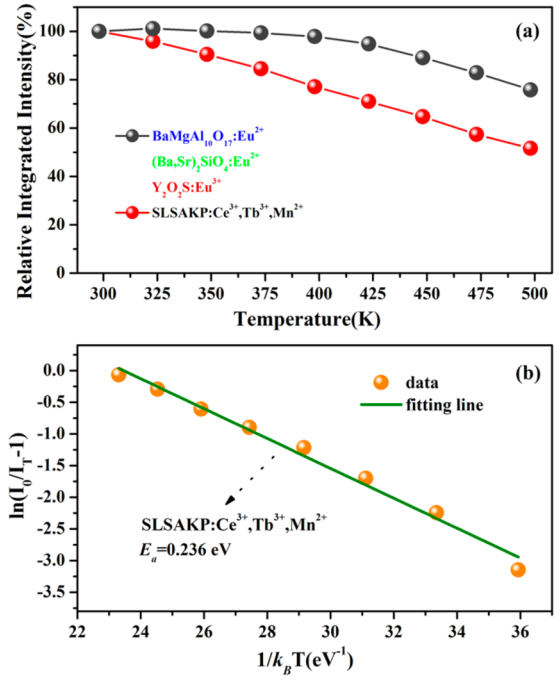

Figure 9. (a) Integrated intensity of the SLSAKP: 0.3%Ce^{3+}, 2.0% Tb^{3+}, 2.0%Mn^{2+} glass and the commercial white-emitting phosphor mixture in the temperature range 298−498 K. (b) Plots of $\ln(I_0/I_T - 1)$ versus $1/k_BT$ for the SLSAKP: 0.3%Ce^{3+}, 2.0%Tb^{3+}, 2.0%Mn^{2+} glass.

From Figure 2c, it is obvious that SLSAKP: 0.3%Ce^{3+}, 1.0% Tb^{3+} shows almost the same PLE features of Ce^{3+} and the characteristic features of Tb^{3+} itself when the $^5D_4$→$^7F_5$ emission (λ_{em} = 542 nm) of Tb^{3+} was monitored. Furthermore, the excitation spectrum (λ_{em} = 542 nm) of SLSAKP: 0.3%Ce^{3+}, 1.0%Tb^{3+} is similar to that (λ_{em} = 407 nm) of the singly Ce^{3+}-

dx.doi.org/10.1021/am405228x | ACS Appl. Mater. Interfaces 2014, 6, 2709−2717

Table 1. CIE Chromaticity Coordinates of Luminescent Glass (SLSAKP: 0.3%Ce^{3+}, 2.0%Tb^{3+}, 2.0%Mn^{2+}) and Commercial White-Emitting Phosphor Mixture under 356 and 370 nm Excitation, Respectively, In the Temperature Range 298−498 K

	CIE coordinates[a]	
T (K)	*A	*B
298	(0.288,0.305)	(0.313,0.316)
323	(0.285,0.308)	(0.319,0.313)
348	(0.282,0.309)	(0.324,0.311)
373	(0.279,0.312)	(0.327,0.307)
398	(0.276,0.316)	(0.328,0.304)
423	(0.273,0.320)	(0.328,0.297)
448	(0.270,0.323)	(0.323,0.286)
473	(0.269,0.330)	(0.320,0.272)
498	(0.267,0.334)	(0.316,0.252)

[a]*A, luminescent glass; *B, commercial white-emitting phosphor mixture.

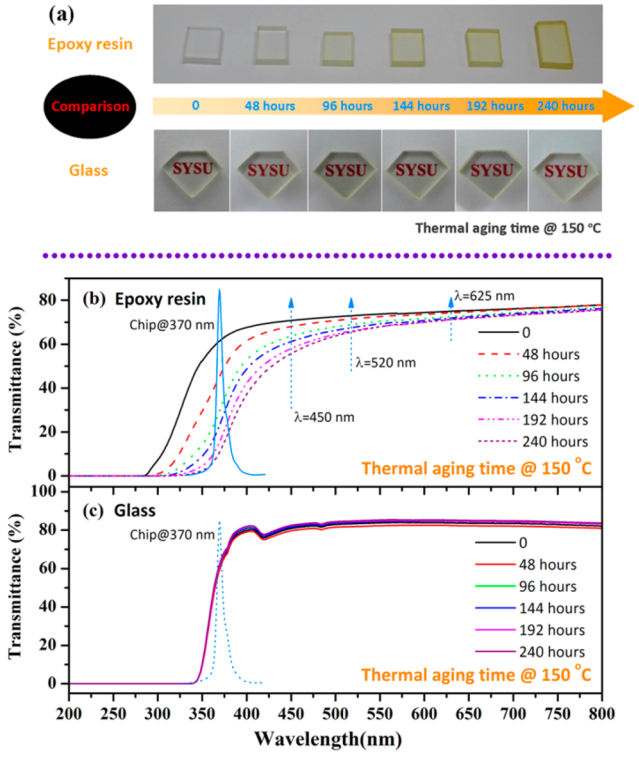

Figure 10. (a) Photographic images of the epoxy resin and the SLSAKP: 0.3%Ce^{3+}, 2.0%Tb^{3+}, 2.0%Mn^{2+} glass after heating at 150 °C for different aging time (t = 0, 48, 96, 144, 192, 240 h). (b) Transmittance spectra of (b) the epoxy resin and (c) the SLSAKP: 0.3%Ce^{3+}, 2.0%Tb^{3+}, 2.0%Mn^{2+} glass after heating at 150 °C for different aging time (t = 0, 48, 96, 144, 192, 240 h).

doped glass. The presence of the Ce^{3+} absorption band in the excitation spectrum of the green emission of Tb^{3+} suggests the existence of an energy transfer process from Ce^{3+} to Tb^{3+} in SLSAKP: 0.3%Ce^{3+}, 1.0%Tb^{3+}.

Figure 3a shows the PL spectra of SLSAKP: 0.3%Ce^{3+}, y%Tb^{3+} (y = 0, 1.0, 2.0, 4.0%) glasses under excitation at 356 nm. The emission spectra contain a blue-violet emission of Ce^{3+} at 407 nm and a series of strong emission lines of Tb^{3+} at 486, 542, 585, and 620 nm. With increasing Tb^{3+} concentration, the emission intensity of Ce^{3+} decreases gradually while the

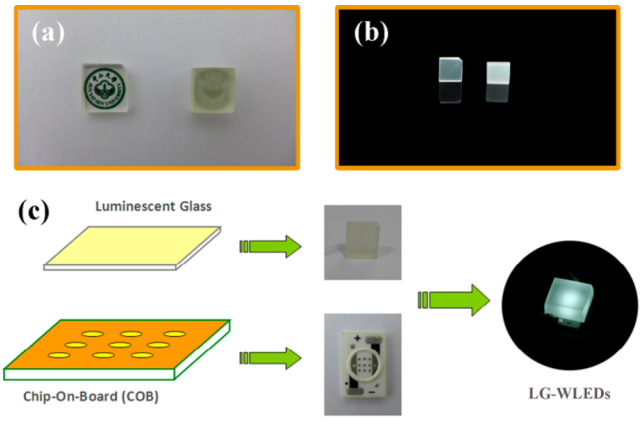

Figure 11. Photographic images of (left) the mirror- and (right) the rough-polished SLSAKP: 0.3%Ce^{3+}, 2.0%Tb^{3+}, 2.0%Mn^{2+} glasses: (a) under white-emitting fluorescent lamp; (b) under 365 nm UV lamp. (c) The conceptual and actual fabrication process of LG-WLEDs based on combination of COB and luminescent glass.

emission intensity of Tb^{3+} increases monotonically. The dependence of the integrated emission intensities of Ce^{3+} and Tb^{3+} on the Tb^{3+} concentration is also shown in the inset of Figure 3a. These results indicate that an efficient energy transfer takes place from Ce^{3+} to Tb^{3+}. Therefore, tunable multicolor emissions from blue-violet light to green light are strongly expected in SLSAKP: 0.3%Ce^{3+}, y%Tb^{3+} glasses through the $Ce^{3+}\rightarrow Tb^{3+}$ energy transfer.

To further evaluate the efficiency of the energy transfer from Ce^{3+} to Tb^{3+}, we measured the decay curves of Ce^{3+} in SLSAKP: 0.3%Ce^{3+}, y%Tb^{3+} and are represented in Figure 3b. The decay curve of SLSAKP: 0.3%Ce^{3+} was well fitted with a typical single exponential function, and the Ce^{3+} lifetime was determined to be about 45.14 ns. With increasing Tb^{3+} concentration, the lifetime of Ce^{3+} ions gradually decreases in SLSAKP: 0.3%Ce^{3+}, y%Tb^{3+} and its values are 42.64 ns for y = 1.0%, 40.85 ns for y = 2.0% and 37.03 ns for y = 4.0%. These results further prove the existence of energy transfer from Ce^{3+} to Tb^{3+}. We also evaluated the energy transfer efficiency. Generally, the efficiency of energy transfer from a sensitizer to an activator can be expressed by the following eq 1[31−33]

$$\eta_T = 1 - \frac{\tau}{\tau_0} \quad (1)$$

where τ_0 and τ are the lifetimes of the sensitizer in the absence and presence of the activator, respectively. The energy transfer efficiency (η_{Ce-Tb}) from Ce^{3+} to Tb^{3+} in SLSAKP: 0.3%Ce^{3+}, y%Tb^{3+} were calculated as a function of Tb^{3+} content and are shown in the inset of Figure 3b. It is clear that η_{Ce-TbI} increases with Tb^{3+} dopant content. The maximum value is about 18% at y = 4.0%.

The PLE and PL spectra of SLSAKP: 0.3%Ce^{3+}, SLSAKP: 0.5%Mn^{2+} and SLSAKP: 0.3%Ce^{3+}, 2.0%Mn^{2+} are shown in Figure 4. In Figure 4b, the emission spectrum of SLSAKP: 0.5% Mn^{2+} shows a broad red emission band centered at 612 nm ascribed to the $^4T_1(^4G)\rightarrow{}^6A_1(^6S)$ transition of Mn^{2+} ions. The excitation spectrum contains three bands centered around 257, 355, and 418 nm, which correspond to the allowed Mn−O charge transfer transition and the two spin-forbidden transitions from $^6A_1(^6S)$ to $^4T_2(^4D)$ and $^4A_1(G)$, $^4E(G)$, respectively.[34] As shown in Figure 4a, the Ce^{3+} emission spectrum shows an overlap with the excitation spectrum of Mn^{2+} in a wavelength

dx.doi.org/10.1021/am405228x | ACS Appl. Mater. Interfaces 2014, 6, 2709−2717

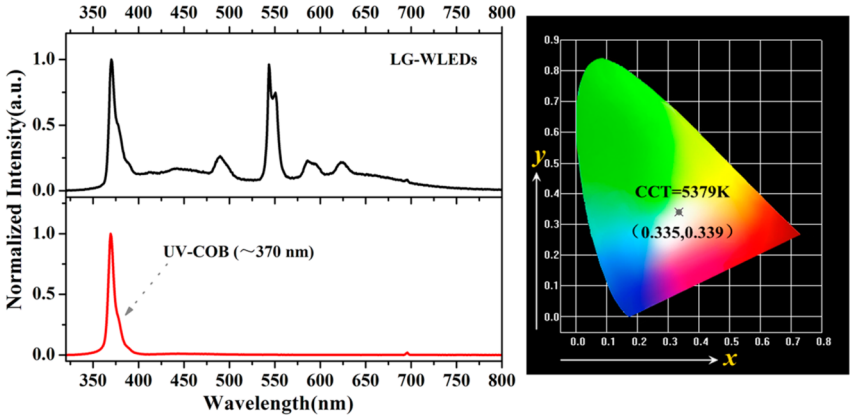

Figure 12. EL spectra (left) and chromaticity diagram (right) of the as-fabricated LG-WLEDs combining SLSAKP: 0.3%Ce^{3+}, 2.0%Tb^{3+}, 2.0%Mn^{2+} glass with UV-COB under an operating current of 40 mA.

range 370−450 nm, which indicates a possible energy transfer from Ce^{3+} to Mn^{2+}. As shown in Figure 4c, the excitation spectrum of the red emission of Mn^{2+} at 612 nm is almost consistent with the typical excitation spectrum of the blue-violet emission of Ce^{3+} at 407 nm, as shown in Figure 4a. This result indicates the occurrence of an energy transfer from Ce^{3+} to Mn^{2+} ions. The excitation intensity of SLSAKP: 0.5%Mn^{2+} was also compared with that of SLSAKP: 0.3%Ce^{3+} under the same measurement conditions. It is obviously seen in Figure 4a that Mn^{2+} shows much lower excitation intensity than Ce^{3+} in the same wavelength range (330−400 nm). This suggests that Ce^{3+} rather than Mn^{2+} is mainly excited under 356 nm UV light. Under the excitation of 356 nm, the emission spectrum of SLSAKP: 0.3%Ce^{3+}, 2.0%Mn^{2+} exhibits an intense blue-violet emission of Ce^{3+} at 407 nm and another weak orange-red band of Mn^{2+} at 620 nm. These results further support the existence of an energy transfer from Ce^{3+} to Mn^{2+} in the SLSAKP: Ce^{3+}, Mn^{2+} glasses. As shown in Supporting Information (Figure S1), the energy transfer efficiency (η_{Ce-Mn}) was also evaluated to be about 22.1% at z = 2.0%, and this value is not high enough. Figure S2 in the Supporting Information simply describes the energy transfer mechanism from Ce^{3+} to Tb^{3+} and Mn^{2+}. Through the energy transfer process between Ce^{3+} and Tb^{3+}/Mn^{2+}, it is possible to obtain white light in the SLSAKP host by codoping the three ions and appropriately adjusting their concentrations.

As shown in the inset of Figure 6, Ce^{3+}, Tb^{3+}, and Mn^{2+} singly doped glasses give blue-violet, green, and orange-red emissions under 365 nm UV lamp irradiation. Their CIE color coordinates were calculated to be about (0.161, 0.077), (0.292, 0.487), and (0.479, 0.480), respectively. On the basis of the above results of energy transfer from Ce^{3+} to Tb^{3+} and Mn^{2+}, it was therefore expected that white light emission may be obtained by simply adjusting the content ratio of Tb^{3+}/Mn^{2+} in Ce^{3+}, Tb^{3+}, and Mn^{2+} triply doped glasses. The PL spectra and CIE chromaticity diagram of the SLSAKP: 0.3%Ce^{3+}, $y$$Tb^{3+}$, $z$$Mn^{2+}$ glasses are shown in Figures 5 and 6, respectively. As shown in Figure 5a, the emission intensity of Mn^{2+} slightly increases and that of Ce^{3+} or Tb^{3+} decreases with increasing Mn^{2+} concentration in SLSAKP: 0.3%Ce^{3+}, 2.0%Tb^{3+}, $z$$Mn^{2+}$. Consequently, the glasses emit tunable light from cyan to white color. As shown in Figure 5b, as the concentration of Tb^{3+} increases, the emission intensity of Tb^{3+} increases, that of Ce^{3+} decreases, and that of Mn^{2+} shows almost no change. Therefore, the emission color of the glasses is tuned from bluish white to white and greenish white. Photographic images of SLSAKP: 0.3%Ce^{3+}, 2.0%Tb^{3+}, 2.0%Mn^{2+} (G3 glass) are shown in the inset of Figure 6. It is clearly seen that SLSAKP: 0.3%Ce^{3+}, 2.0%Tb^{3+}, 2.0%Mn^{2+} emits an intense white light under 365 nm UV lamp irradiation. The QE of this glass was recorded using an integrating sphere attached to the FSP920. QE is defined as the ratio of the number of emitted photons (I_{em}) to the number of absorbed photons (I_{abs}), and can be calculated by the following eq 2[16,35]

$$QE = \frac{I_{em}}{I_{abs}} = \frac{\int L_S}{\int E_R - \int E_S} \quad (2)$$

where E_R, E_S are the spectra of the excitation light without and with the sample in the integrating sphere, respectively, and L_S is the luminescence emission spectrum of the sample in the integrating sphere. All the recorded spectroscopic data were corrected with the correction files supplied by the manufacturer. The QE of the SLSAKP: 0.3%Ce^{3+}, 2.0%Tb^{3+}, 2.0%Mn^{2+} glass was measured and calculated to be about 19% under 356 nm excitation.

3.2. Thermal Behaviors of Dual Functional SLSAKP: $x$$Ce^{3+}$, $y$$Tb^{3+}$, $z$$Mn^{2+}$ Glasses as Luminescent Convertor and Encapsulating Material. The thermal quenching properties of luminescent materials are one of the major considerations for their practical application in high-power WLEDs. Figure 7 shows the temperature dependences of the emission spectra and the chromaticity shift of SLSAKP: 0.3% Ce^{3+}, 2.0%Tb^{3+}, 2.0%Mn^{2+} under 356 nm excitation and a commercial white-emitting phosphor mixture under 370 nm excitation. With increasing temperature, the integrated emission intensity of both the SLSAKP: 0.3%Ce^{3+}, 2.0%Tb^{3+}, 2.0%Mn^{2+} glass and the commercial white-emitting phosphor powder gradually decreases as shown in Figure 9a. At 373 and 423 K, the emission intensity of the glass remains about 84.56 and 71.02%, of that observed at 298 K, respectively. Comparatively, the commercial tricolor phosphor mixture maintains higher thermal stability, with about 99.35 and 94.81% white emission intensity at 373 and 423 K, respectively, of that at 298 K. We also determined the activation energy for thermal quenching. The activation energy (E_a) can be expressed by eq 3[36,37]

$$I_T = \frac{I_0}{1 + A\exp\left(-\frac{E_a}{k_B T}\right)} \quad (3)$$

dx.doi.org/10.1021/am405228x | ACS Appl. Mater. Interfaces 2014, 6, 2709−2717

where I_0 is the initial emission intensity, I_T is the intensity at different temperatures, E_a is activation energy of thermal quenching, A is a constant, and k_B is the Boltzmann constant (8.617×10^{-5} eV/K). The E_a for the SLSAKP: 0.3%Ce^{3+}, 2.0% Tb^{3+}, 2.0%Mn^{2+} glass sample was determined to be ~0.236 eV.

As shown in Figure 7c, both the SLSAKP: 0.3%Ce^{3+}, 2.0% Tb^{3+}, 2.0%Mn^{2+} glass and the commercial white-emitting phosphor powder show a slight chromaticity shift with increasing temperature. The CIE chromaticity coordinates of SLSAKP: 0.3%Ce^{3+}, 2.0%Tb^{3+}, 2.0%Mn^{2+} glass with 365 nm excitation and commercial white-emitting phosphor mixture under 370 nm excitation in the temperature range 298−498 K are summarized in Table 1. The former shows higher thermal stability than the latter. The chromaticity shift (ΔE) was calculated using the following eq 4[38]

$$\Delta E = \sqrt{(u'_t - u'_o)^2 + (v'_t - v'_o)^2 + (w'_t - w'_o)^2} \quad (4)$$

where $u' = 4x/(3 - 2x + 12y)$, $v' = 9y/(3 - 2x + 12y)$, and $w' = 1 - u' - v'$. u' and v' are the chromaticity coordinates in $u'v'$ uniform color space, x and y are the chromaticity coordinates in CIE 1931 color space, and o and t are the chromaticity shift at 298 K and a given temperature, respectively. As shown in Figure 8, the chromaticity shift of SLSAKP: 0.3%Ce^{3+}, 2.0% Tb^{3+}, 2.0%Mn^{2+} is 2.94×10^{-2} at 498 K, only 57% of that of the triple-color white-emitting phosphor mixture at the same temperature. This serious chromaticity shift of the commercial white-emitting phosphor mixture is caused by the large differences in the thermal quenching behaviors of rare earth luminescent ions in different hosts, as shown in Figure S3 in the Supporting Information.

As an alternative to epoxy resin as an encapsulating material in WLEDs, the glasses should have high transparency and thermal conductivity at the high junction temperature of high-power LED chips for general lighting applications. Figure 10 shows photographic images and the transmittance spectra of the epoxy resin and the SLSAKP: 0.3%Ce^{3+}, 2.0%Tb^{3+}, 2.0% Mn^{2+} glass after thermal aging at 150 °C for different durations. In Figure 10a, it is obvious that the epoxy resin gradually becomes more and more brown as the thermal aging time increases, owing to the irreversible oxidation of the organic compounds.[9] In contrast, the glass exhibits almost no change in body color. The differences in body color between the SLSAKP: 0.3%Ce^{3+}, 2.0%Tb^{3+}, 2.0%Mn^{2+} glass and epoxy resin are directly associated with the differences in their transmittance spectra. As shown in Figure 10b, as the thermal aging time increases, the absorption edge of the epoxy resin exhibits obvious red shift, whereas the glass shows almost no shift. Furthermore, it is clearly seen in Figure 10b that as the thermal aging time increases, the transmittance of the epoxy resin decreases across the whole wavelength range of 300−800 nm, whereas the glass shows only a tiny decrease. At the 370 nm emission of the UV-COB, the SLSAKP: Ce^{3+}, Tb^{3+}, Mn^{2+} glass shows no transmittance loss while the epoxy resin exhibits 61.62% transmittance at t = 0 and 11.09% at t = 240 h. In other words, the epoxy resin exhibits 82% transmittance loss after thermal aging at 150 °C for 240 h. These results indicate that the thermal aged epoxy resin will compete with the phosphor to absorb the 370 nm emission from the UV-COB and will absorb the visible emissions from the phosphor, which will seriously degrade the total luminous efficiency of the WLEDs at high junction temperature. Comparatively, the as-synthesized glass shows excellent heat-resistance performance. In addition, the luminous efficiency of the UV-COB will seriously decrease at high junction temperature in general.[9,39] Therefore, it is important for WLEDs to conduct heat at large drive current. We thus also measured the thermal conductivity of the SLSAKP: 0.3%Ce^{3+}, 2.0%Tb^{3+}, 2.0%Mn^{2+} glass and the epoxy resin. The thermal conductivity of the glass is 1.07 W/mK, six times larger than that of the epoxy resin (0.17 W/mK),[40] which is important for UV-COB to conduct heat away and consequently maintain a high efficiency and stable chromaticity of the WLEDs. In summary, the white-emitting glass shows good heat-resistance behavior, excellent thermal aging behavior and high thermal conductivity. Therefore, it is strongly expected to be an alternative to epoxy resin as an encapsulating material in high-power WLEDs.

3.3. Fabrication of Organic-Resin-Free LG-WLEDs Based on SLSAKP: *x*Ce^{3+}, *y*Tb^{3+}, *z*Mn^{2+} glasses. Figure 11 (a, left) and (b, left) show the photographic images of the polished SLSAKP: 0.3%Ce^{3+}, 2.0%Tb^{3+}, 2.0%Mn^{2+} glass sample under white-emitting fluorescent lamp and 365 nm UV lamp, respectively. The glass shows high transparency under the white-emitting fluorescent lamp and gives brighter white light at the edges than in the middle under 365 nm UV lamp irradiation. After treatment, the surface of the glass becomes rough and the glass is not very transparent as shown in Figure 11 (a, right), and as-treated glass gives an almost homogeneous white light emission as shown in Figure 11 (b, right), which is extremely important for WLEDs to be used in general lighting. To further demonstrate the potential application of SLSAKP: Ce^{3+}, Tb^{3+}, Mn^{2+} glass, we fabricated a WLEDs prototype by simply placing a plate of the SLSAKP: 0.3%Ce^{3+}, 2.0%Tb^{3+}, 2.0%Mn^{2+} glass on a UV-COB (3 × 3 multiple UV-LED chips) excitation source. Figure 11c illustrates the conceptual and actual fabrication process of the LG-WLEDs. It is clearly seen that the device prototype emits uniform white light at 40 mA forward-bias current (I_F). Figure 12 (left) shows the electroluminescence (EL) spectra of the naked UV-COB and LG-WLEDs under I_F = 40 mA. The EL spectra show a UV band at around 370 nm, which belongs to UV-COB, and several emission bands and peaks in the 400−800 nm region, where blue-violet emission centered at 407 nm is ascribed to Ce^{3+}, green emission centered at 486, 542, 585, and 620 nm owing to Tb^{3+}, and orange-red emission centered at 620 nm from Mn^{2+} ions. It is also seen in Figure 12 (left) that intense UV light passes through the glass, which is harmful to human body in practical application. Therefore, to enhance the absorption in UV wavelength region, glass-ceramic may be obtained via well-controlled thermal treatment for the as-synthesized glass, which is under our future consideration. As illustrated in Figure 12 (right), the CIE color coordinates and CCT of the as-fabricated LG-WLEDs are (x = 0.335, y = 0.339), 5379 K under I_F = 40 mA, which is close to ideal white light.

4. CONCLUSION

In conclusion, we have synthesized a series of novel bifunctional single-component white-emitting SLSAKP: *x*Ce^{3+}, *y*Tb^{3+}, *z*Mn^{2+} glasses by utilizing the principle of energy transfer and properly adjusting the activator contents via the conventional melt-quenching method. These glasses are able to serve as both luminescent convertor and encapsulating material in pc-WLEDs. The as-synthesized SLSAKP: 0.3%Ce^{3+}, 2.0% Tb^{3+}, 2.0%Mn^{2+} glass shows good thermal stability, inconspicuous chromaticity shift, better high-temperature resistance, and higher thermal conductivity. These are rare but desirable

characteristics that are not present in the phosphors used as luminescent convertor and the epoxy resin used as the encapsulating material in pc-WLEDs. LG-WLEDs based on SLSAKP: 0.3%Ce^{3+}, 2.0%Tb^{3+}, 2.0%Mn^{2+} glass and UV-COB was successfully fabricated, and the CIE color coordinates and CCT of the as-fabricated LG-WLEDs are (0.335, 0.339) and 5379 K, respectively. These results indicate that SLSAKP: Ce^{3+}, Tb^{3+}, Mn^{2+} glass may serve as a potential bifunctional white-light-emitting material for LG-WLEDs pumped by UV-LED chips, especially high-power UV-COB.

■ ASSOCIATED CONTENT

Supporting Information

Decay curves (λ_{ex} = 356 nm, λ_{em} = 407 nm) of Ce^{3+} in SLSAKP: 0.3% Ce^{3+}, zMn^{2+} (z = 0, 0.5, 1.0, 2.0%) (Figure S1); schematic diagram of energy transfer from Ce^{3+} to Tb^{3+} and Mn^{2+} in SLSAKP: Ce^{3+}, Tb^{3+}, Mn^{2+} glass (Figure S2); temperature-dependent PL spectra of (a) $BaMgAl_{10}O_{17}$: Eu^{2+}, (b) $(Ba,Sr)_2SiO_4$: Eu^{2+}, and (c) Y_2O_2S: Eu^{3+} phosphors excited at 370 nm (Figure S3). This material is available free of charge via the Internet at http://pubs.acs.org.

■ AUTHOR INFORMATION

Corresponding Author

*E-mail: ceswj@mail.sysu.edu.cn. Tel: +86-20-84112112. Fax: +86-20-84111038.

Notes

The authors declare no competing financial interest.

■ ACKNOWLEDGMENTS

This work was financially supported by the "973" programs (2014CB643801), the NSFC (21271191, 20971130), the Joint Funds of the National Natural Science Foundation of China and Guangdong Province (U1301242), Teamwork Projects of Guangdong Natural Science Foundation (S2013030012842), Guangdong Provincial and Guangzhou Science & Technology Project (2012A080106005, 2013Y2-00118, 11A34041302), and the LED Industry Development Project of Jiangmen (No. [2011]231-201111).

■ REFERENCES

(1) Lin, C. C.; Liu, R. S. Advances in Phosphors for Light-Emitting Diodes. *J. Phys. Chem. Lett.* **2011**, *2*, 1268−1277.

(2) Feldmann, C.; Jüstel, T.; Ronda, C. R.; Schmidt, P. J. Inorganic Luminescent Materials: 100 Years of Research and Application. *Adv. Funct. Mater.* **2003**, *13*, 511−516.

(3) Pimputkar, S.; Speck, J. S.; DenBaars, S. P.; Nakamura, S. Prospects for LED Lighting. *Nat. Photonics* **2009**, *3*, 180−182.

(4) Höppe, H. A. Recent Developments in the Field of Inorganic Phosphors. *Angew. Chem., Int. Ed.* **2009**, *48*, 3572−3582.

(5) Schubert, E. F.; Kim, J. K. Solid-State Light Sources Getting Smart. *Science* **2005**, *308*, 1274−1278.

(6) Peng, M.; Yin, X.; Tanner, P. A.; Liang, C.; Li, P.; Zhang, Q.; Qiu, J. Orderly-Layered Tetravalent Manganese-Doped Strontium Aluminate $Sr_4Al_{14}O_{25}$:Mn^{4+}: An Efficient Red Phosphor for Warm White Light Emitting Diodes. *J. Am. Ceram. Soc.* **2013**, *96*, 2870−2876.

(7) Chang, M. H.; Das, D.; Varde, P. V.; Pecht, M. Light Emitting Diodes Reliability Review. *Microelectron. Reliab.* **2012**, *52*, 762−782.

(8) Nakanishi, T.; Tanabe, S. Novel Eu^{2+}-Activated Glass Ceramics Precipitated With Green and Red Phosphors for High-Power White LED. *IEEE J. Sel. Top. Quantum Electron.* **2009**, *15*, 1171−1176.

(9) Lafont, U.; van Zeijl, H.; van der Zwaag, S. Increasing the Reliability of Solid State Lighting Systems via Self-Healing Approaches: A Review. *Microelectron. Reliab.* **2012**, *52*, 71−89.

(10) Ha, M.; Graham, S. Development of A Thermal Resistance Model for Chip-On-Board Packaging of High Power LED Arrays. *Microelectron. Reliab.* **2012**, *52*, 836−844.

(11) Cui, Z.; Ye, R.; Deng, D.; Hua, Y.; Zhao, S.; Jia, G.; Li, C.; Xu, S. Eu^{2+}/Sm^{3+} Ions Co-doped White Light Luminescence $SrSiO_3$ Glass-Ceramics Phosphor for White LED. *J. Alloys Compd.* **2011**, *509*, 3553−3558.

(12) Schubert, E. F.; Kim, J. K.; Luo, H.; Xi, J.-Q. Solid-State Lighting-A Benevolent Technology. *Rep. Prog. Phys.* **2006**, *69*, 3069−3099.

(13) Wondraczek, L.; Krolikowski, S.; Nass, P. Europium Partitioning, Luminescence Re-absorption and Quantum Efficiency in (Sr,Ca) åkermanite-feldspar Bi-Phasic Glass Ceramics. *J. Mater. Chem. C* **2013**, *1*, 4078−4086.

(14) Zeng, H.; Yu, Q.; Wang, Z.; Sun, L.; Ren, J.; Chen, G.; Qiu, J. Tunable Multicolor Emission and Energy Transfer of Sb^{3+}/Mn^{2+} Codoped Phosphate Glasses by Design. *J. Am. Ceram. Soc.* **2013**, *96*, 2476−2480.

(15) Chen, D.; Yu, Y.; Lin, H.; Huang, P.; Weng, F.; Shan, Z.; Wang, Y. CeF_3-based Glass Ceramic: A Potential Luminescent Host for White-Light-Emitting diode. *Opt. Lett.* **2009**, *34*, 2882−2884.

(16) Zhang, R.; Lin, H.; Yu, Y.; Chen, D.; Xu, J.; Wang, Y. A New-Generation Color Converter for High-Power White LED: Transparent Ce^{3+}: YAG Phosphor-in-Glass. *Laser Photon. Rev.* **2014**, *8*, 158−164.

(17) Fujita, S.; Yoshihara, S.; Sakamoto, A.; Yamamoto, S.; Tanabe, S. YAG Glass-Ceramic Phosphor for White LED (I): Background and Development. *Proc. SPIE* **2005**, *5941*, 594111−7.

(18) Tanabe, S.; Fujita, S.; Yoshihara, S.; Sakamoto, A.; Yamamoto, S. YAG Glass-Ceramic Phosphor for White LED (II): Luminescence Characteristics. *Proc. SPIE* **2005**, *5941*, 594112−6.

(19) Liu, Z.; Yu, Y.; Dai, N.; Chen, Q.; Yang, L.; Li, J.; Qiao, Y. Super Broadband Reddish Emitting Glass with Eu^{2+} Doped for Warm-White Light-Emitting Diodes. *Appl. Phys. A: Mater. Sci. Process.* **2012**, *108*, 777−781.

(20) Lima, S. M.; da Cunha Andrade, L. H.; Silva, J. R.; Bento, A. C.; Baesso, M. L.; Sampaio, J. A.; de Oliveira Nunes, L. A.; Guyot, Y.; Boulon, G. Broad Combined Orange-red Emissions from Eu^{2+}- and Eu^{3+}-Doped Low-Silica Calcium Aluminosilicate Glass. *Opt. Express* **2012**, *20*, 12658−12665.

(21) Ming, C.; Song, F.; Li, C.; Yu, Y.; Zhang, G.; Yu, H.; Sun, T.; Tian, J. Highly Efficient Downconversion White Light in Tm^{3+}/Tb^{3+}/Mn^{2+} Tridoped P_2O_5-Li_2O-Sb_2O_3 Glass. *Opt. Lett.* **2011**, *36*, 2242−2244.

(22) Song, F.; Ming, C.; An, L.; Wang, Q.; Yu, Y.; Yu, H.; Sun, T.; Tian, J. Tm^{3+}/Tb^{3+}/Mn^{2+} Tri-doped Phosphate Glass Ceramic for Enhanced White-Light-Emitting Material. *Mater. Lett.* **2011**, *65*, 3140−3142.

(23) Zhu, Z.; Zhang, Y.; Qiao, Y.; Liu, H.; Liu, D. Luminescence Properties of Ce^{3+}/Tb^{3+}/Sm^{3+} Co-doped CaO-SiO_2-B_2O_3 Glasses for White Light Emitting Diodes. *J. Lumin.* **2013**, *134*, 724−728.

(24) Zhang, Y.; Zhu, Z.; Qiao, Y. Luminescence Properties of Ce^{3+}/Tb^{3+}/Eu^{3+} Triply-doped CaO-B_2O_3-SiO_2 Glasses for White Light Emitting Diodes. *Mater. Lett.* **2013**, *93*, 9−11.

(25) Zhu, C.; Yang, Y.; Liang, X.; Yuan, S.; Chen, G. Rare Earth Ions Doped Full-Color Luminescence Glasses for White LED. *J. Lumin.* **2007**, *126*, 707−710.

(26) Zhang, J. C.; Parent, C.; Le Flem, G.; Hagenmuller, P. White Light Emitting Glass. *J. Solid State Chem.* **1991**, *93*, 17−29.

(27) Martínez-Martínez, R.; Speghini, A.; Bettinelli, M.; Falcony, C.; Caldiño, U. White Light Generation Through the Zinc Metaphosphate Glass Activated by Ce^{3+}, Tb^{3+} and Mn^{2+} Ions. *J. Lumin.* **2009**, *129*, 1276−1280.

(28) Yu, Y.; Liu, Z.; Dai, N.; Sheng, Y.; Luan, H.; Peng, J.; Jiang, Z.; Li, H.; Li, J.; Yang, L. Ce-Tb-Mn Co-doped White Light Emitting Glasses Suitable for Long-Wavelength UV Excitation. *Opt. Express* **2011**, *19*, 19473−19479.

(29) Sontakke, A. D.; Biswas, K. Annapurna, K. Concentration-dependent Luminescence of Tb^{3+} Ions in High Calcium Aluminosilicate Glasses. *J. Lumin.* **2009**, *129*, 1347−1355.

(30) Blasse, G.; Grabmaier, B. C. In *Luminescent Materials*; Springer: Berlin, 1994; Chapter 3, pp 33−70.
(31) Paulose, P. I.; Jose, G.; Thomas, V.; Unnikrishnan, N. V.; Warrier, M. K. R. Sensitized Fluorescence of Ce^{3+}/Mn^{2+} System in Phosphate Glass. *J. Phys. Chem. Solids* **2003**, *64*, 841−846.
(32) Huang, C.-H.; Chen, T.-M.; Liu, W.-R.; Chiu, Y.-C.; Yeh, Y.-T.; Jang, S.-M. A Single-Phased Emission-Tunable Phosphor $Ca_9Y(PO_4)_7:Eu^{2+},Mn^{2+}$ with Efficient Energy Transfer for White-Light-Emitting Diodes. *ACS Appl. Mater. Interfaces* **2010**, *2*, 259−264.
(33) Li, G.; Zhang, Y.; Geng, D.; Shang, M.; Peng, C.; Cheng, Z.; Lin, J. Single-Composition Trichromatic White-Emitting $Ca_4Y_6(SiO_4)_6O:Ce^{3+}/Mn^{2+}/Tb^{3+}$ Phosphor: Luminescence and Energy Transfer. *ACS Appl. Mater. Interfaces* **2012**, *4*, 296−305.
(34) Lin, H.; Zhang, R.; Chen, D.; Yu, Y.; Yang, A.; Wang, Y. Tuning of Multicolor Emissions in Glass Ceramics Containing γ-Ga_2O_3 and β-YF_3 Nanocrystals. *J. Mater. Chem. C* **2013**, *1*, 1804−1811.
(35) Lin, H.; Chen, D.; Yu, Y.; Zhang, R.; Wang, Y. Molecular-like Ag Clusters Sensitized Near-Infrared Down-Conversion Luminescence in Oxyfluoride Glasses for Broadband Spectral Modification. *Appl. Phys. Lett.* **2013**, *103*, 091902−091905.
(36) Baginskiy, I.; Liu, R. S. Significant Improved Luminescence Intensity of Eu^{2+}-doped $Ca_3SiO_4Cl_2$ Green Phosphor for White LEDs Synthesized Through Two-Stage Method. *J. Electrochem. Soc.* **2009**, *156*, 29−32.
(37) Geng, D.; Shang, M.; Zhang, Y.; Lian, H.; Cheng, Z.; Lin, J. Tunable Luminescence and Energy Transfer Properties of $Ca_5(PO_4)_2SiO_4:Ce^{3+}/Tb^{3+}/Mn^{2+}$ Phosphors. *J. Mater. Chem. C* **2013**, *1*, 2345−2353.
(38) Tsai, C.-C.; Cheng, W.-C.; Chang, J.-K.; Chen, L.-Y.; Chen, J.-H.; Hsu, Y.-C.; Cheng, W.-H. Ultra-High Thermal-Stable Glass Phosphor Layer for Phosphor-Converted White Light-Emitting Diodes. *J. Disp. Technol.* **2013**, *9*, 427−432.
(39) Chhajed, S.; Xi, Y.; Li, Y.-L.; Gessmann, Th.; Schubert, E. F. Influence of Junction Temperature on Chromaticity and Color-Rendering Properties of Trichromatic White-Light Sources Based on Light-Emitting Diodes. *J. Appl. Phys.* **2005**, *97*, 054506−054513.
(40) Christensen, A.; Graham, S. Thermal Effects in Packaging High Power Light Emitting Diode Arrays. *Appl. Therm. Eng.* **2009**, *29*, 364−371.